






Sound scattering by a bubble metasurface

Gyani Shankar Sharma ^{1,*}, Alex Skvortsov ², Ian MacGillivray ², and Nicole Kessissoglou ¹

¹*School of Mechanical and Manufacturing Engineering, University of New South Wales, Sydney, New South Wales 2052, Australia*

²*Maritime Division, Defence Science and Technology, Melbourne, Victoria 3207, Australia*

 (Received 28 July 2020; revised 30 November 2020; accepted 2 December 2020; published 21 December 2020)

We present an analytical framework to investigate the acoustic performance of an array of closely spaced spherical cavities embedded in a thin soft medium submerged in water. Each layer of cavities is approximated as a homogenized layer with effective properties. Strong monopole resonance of the cavities and multiple scattering of waves between cavities in proximity are taken into account. Analytical results for the metasurface with and without a rigid backing are compared with numerical simulations as well as with experimental results from the literature.

DOI: [10.1103/PhysRevB.102.214308](https://doi.org/10.1103/PhysRevB.102.214308)

I. INTRODUCTION

A metasurface is a planar device with the ability to manipulate waves of wavelength much longer than its thickness, arising from the interaction between an incident wave and its rationally designed architecture [1–4]. A metasurface comprising a soft medium embedded with cavities is a favorable candidate to control water-borne sound waves, attributed to impedance matching of the soft medium with water and strong monopole resonance of the cavities. Multiple scattering of waves between cavities in proximity further strengthens the resonance, leading to enhanced wave manipulation that blocks transmission [5–7] or perfectly absorbs [8,9] sound waves. Similar metasurface designs have been used for sub-wavelength focusing [10,11], wave guiding [12], localization [13,14], and the generation of band gaps [15,16], negative dynamic density, and elastic modulus [17,18]. Existing analytical models of cavities in a soft medium are valid for low and moderate filling fraction values [5,8,19,20]. These models predict that optimal sound absorption by a bubble metasurface can be achieved at moderate filling fraction values [8]. We herein show that a soft material with a layer of closely spaced cavities can effectively block the sound transmission. While anechoic coatings comprising moderately spaced cavities in a soft medium are effective in absorbing water-borne sound, decoupling coatings comprising proximal cavities in a soft medium can be effective in reducing the transmission of structure-borne sound [21].

Due to the complexity of wave phenomena in metasurfaces arising from multiple scattering, local resonances, and resonance coupling, their analytical modeling is often a challenging undertaking; for example, see [22–26]. The effective medium approximation is a powerful method for simplified modeling of complex media in the long-wavelength limit, whereby an inhomogeneous medium is approximated as a homogeneous medium with effective properties [27,28]. A

key challenge for homogenization of a strongly scattering composite such as closely spaced cavities in a soft medium arises from coupling between the resonators as a result of multiple scattering of waves [24,29]. This challenge is addressed here.

We present an effective medium approximation formulation for a metasurface formed by a lattice of closely spaced spherical cavities embedded in a thin soft medium, as shown in Fig. 1(a). Each layer of cavities in the direction of sound propagation is approximated as a homogenized layer of fluid for which we derive an effective thickness in addition to effective fluid properties, as shown in Fig. 1(b). The homogenized layer is considered as a structured element and integrated into a more complex layer structure that is treated using the conventional transfer matrix method. The proposed model explicitly accounts for multiple scattering effects between cavities. We validate our analytical results with numerical simulations and with experimental data from the literature.

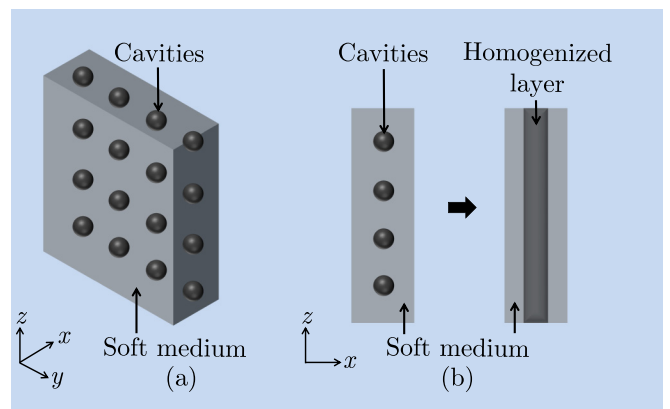


FIG. 1. Schematic diagram showing (a) a layer of spherical cavities in a soft material and (b) the layer of cavities approximated as a homogenized layer with effective properties. The soft medium embedded with cavities is submerged in water and subject to acoustic plane-wave excitation in the x direction.

*gyanishankar.sharma@unsw.edu.au

II. EFFECTIVE MEDIUM APPROXIMATION

The soft elastic medium has density ρ , shear modulus $\mu = \mu' + i\mu''$, and longitudinal modulus $\kappa = \kappa' + i\kappa''$, where $\mu \ll \kappa$. In an unbounded medium, the monopole resonance frequency of a single evacuated spherical inclusion of radius a is given by [30]

$$\omega_0 = 2 \frac{c_s}{a}, \quad (1)$$

where $c_s = \sqrt{\mu'/\rho}$ is the shear wave speed. The wavelength corresponding to the monopole resonance is much larger than the inclusion size as a direct consequence of the softness of the medium, since $\omega_0 a / c_l = 2c_s / c_l \ll 1$ and $c_l = \sqrt{\kappa/\rho}$ is the longitudinal wave speed. Therefore, a lattice of cavities in a soft medium can be well described within the effective medium approximation framework.

Consider an array of spherical cavities with lattice spacing d_x in the direction of sound propagation and lattice spacing $d_y = d_z$ in the lateral directions. The density ρ_e and longitudinal modulus κ_e of the effective medium due to homogenization of a layer of cavities in the direction of sound propagation are given by the following conservation equations [31]:

$$\langle \rho \rangle = \rho_e (l_e / d_x) + \rho [1 - (l_e / d_x)], \quad (2)$$

$$\frac{1}{\langle \kappa \rangle} = \frac{(l_e / d_x)}{\kappa_e} + \frac{1 - (l_e / d_x)}{\kappa}, \quad (3)$$

where l_e is the effective thickness of the homogenized layer, and $\langle \rho \rangle$ and $\langle \kappa \rangle$ are, respectively, the density and longitudinal modulus averaged over the unit cell comprising a single cavity at the center of a cuboidal soft medium of volume $d_x d_y^2$.

The thickness of the layer due to homogenization of cavities is related to the so-called blockage length, which has been characterized using potential flow perturbation by a grating of obstacles [32]. The low and high filling fraction limits of the blockage length for rigid spheres in potential flow have previously been derived as [33]

$$l_{e,\text{low}} = 2\pi a \left(\frac{a}{d_y} \right)^2, \quad (4)$$

$$l_{e,\text{high}} = \frac{\pi \sqrt{2}}{2} \frac{a}{\sqrt{(1/\zeta) - 1}}, \quad (5)$$

where $\zeta = \sqrt{\pi} a / d_y$. These expressions are also valid for a lattice of bubbles at small amplitude oscillations [34]. An interpolation function for the blockage length is obtained as a weighted sum of the blockage length at low and high filling fraction using

$$l_e = (1 - \zeta^\beta) l_{e,\text{low}} + \zeta^\beta l_{e,\text{high}}. \quad (6)$$

We have used the power exponent of $\beta = 12$ in the interpolation function to reduce the contribution of the blockage length at high filling fraction.

The averaged density is given by [35]

$$\langle \rho \rangle = \rho(1 - \alpha), \quad (7)$$

where $\alpha = 4\pi a^3 / 3d_x d_y^2$ is the filling fraction of cavities in the matrix. We derive the averaged longitudinal modulus using

the sound speed in a bubble mixture [19,36,37] as

$$\langle \kappa \rangle = \frac{\kappa(1 - \alpha)}{1 + 4\pi\kappa f_s / \rho\omega^2 d_x d_y^2}, \quad (8)$$

where

$$f_s = \frac{a}{(\omega_0/\omega)^2 - I + i\delta} \quad (9)$$

is the scattering function of an array of spherical cavities and $\delta = 4\mu'' / \rho\omega^2 a^2$ is the viscous damping of a spherical cavity [20]. We have used the time convention $e^{i\omega t}$, where $i = \sqrt{-1}$, ω is the excitation frequency, and t is time. Parameter I accounts for multiple scattering effects between the spherical cavities, whereby $I = 1$ corresponds to single scattering approximation [20]. There are a number of expressions for parameter I available in the literature [19,20,38], which are valid for low and moderate filling fraction values. In this study, we use

$$I = \exp(-2\pi a / d_y), \quad (10)$$

which can be derived from the following scaling arguments. Since the resonance frequency scales with the inverse of the square root of the added mass [39] and the resonance of an array of cavities occurs at ω_0 / \sqrt{I} [19,20], parameter I can also be expressed as

$$I = \frac{M}{m_0}, \quad (11)$$

where m_0 is the added mass of a pulsating cavity in an unbounded medium and M is the added mass of the same cavity in an array. The added mass of a cavity in the lattice is equivalent to the added mass of a monopolar resonator in a square duct of cross section d_y^2 . The ratio of the added mass of a monopolar resonator in a square duct to that of the same resonator in an unbounded domain is given by [40]

$$\frac{M}{m_0} = \frac{4a}{d_y} \sum_{n=0, m=1}^{\infty} \frac{\exp[-2\pi(a/d_y)\sqrt{n^2 + m^2}]}{\sqrt{n^2 + m^2}}, \quad (12)$$

where integer indices n, m define the position of all monopole resonators in the lattice. It should be noted that in the long-wavelength limit, the compressibility disappears from the expression of the added mass of a monopole resonator in a duct. In this limit, the added mass reduces to a function of geometrical parameters only [40]. Evaluating the lattice sum in Eq. (12) by converting it to an integral as described in Ref. [41], we arrive at Eq. (10).

Substituting Eqs. (7) and (8) into Eqs. (2) and (3), we obtain the following expressions for the effective density and longitudinal modulus of the homogenized layer:

$$\rho_e = \rho(1 - \alpha d_x / l_e), \quad (13)$$

$$\kappa_e = \frac{\kappa(1 - \alpha)}{\frac{\alpha d_x}{l_e} \left(1 + \frac{3\kappa}{\rho\omega^2 a^3} f_s \right) + (1 - \alpha)}. \quad (14)$$

The effective wave number and impedance of the homogenized layer are obtained as $k_e = \omega \sqrt{\rho_e / \kappa_e}$ and $Z_e = \sqrt{\rho_e \kappa_e}$. Similarly, the wave number and impedance of the elastic medium are calculated using $k = \omega \sqrt{\rho / \kappa}$ and $Z = \sqrt{\rho \kappa}$. The transfer matrix for each layer is then determined using the

pertinent thickness, impedance, and wave number. The global transfer matrix is obtained by multiplying the transfer matrices for the various layers in their order of appearance in the direction of sound propagation [42]. The transmission, reflection, and absorption coefficients are calculated using the elements of the global transfer matrix and impedances of the media on the incidence and transmission sides of the metasurface [42].

III. NUMERICAL MODEL

For validation of the proposed framework, analytical results are compared with numerical simulations as well as with experimental data from the literature. The numerical simulations were performed using COMSOL MULTIPHYSICS in which the elastic medium was modeled using the SOLID MECHANICS module and water was modeled using the PRESSURE ACOUSTICS module. Interactions between the solid and fluid domains were simulated by applying acoustic-structure boundary conditions at the interface. A free boundary condition was applied at the interface between the cavities and the elastic medium. Periodicity of the cavities was simulated using periodic boundary conditions. An incident acoustic pressure of unity amplitude was applied using the background pressure field. Anechoic termination of outgoing waves was simulated using a perfectly matched layer. Reflected and transmitted pressures were, respectively, measured at a plane on the incidence and transmission sides of the metasurface.

IV. RESULTS AND DISCUSSION

The effect of multiple scattering of waves between spherical cavities on the monopole resonance frequency is initially examined. Figure 2 presents parameter I as a function of the ratio of cavity radius to lattice spacing, a/d_y . The limits $a/d_y = 0$ and $a/d_y = 0.5$, respectively, correspond to a single

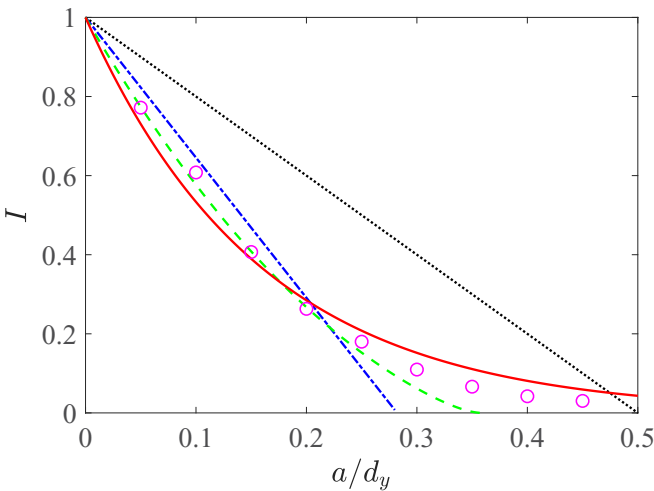


FIG. 2. Parameter I for a square lattice of spherical cavities obtained using Eq. (10) (solid red line) and numerically using the finite-element method (magenta circles). Our analytical and numerical results are compared with Kobelev [38] (dotted black line), Leroy *et al.* [19] (dash-dotted blue line), and Skvortsov *et al.* [20] (dashed green line).

TABLE I. Expressions for multiple scattering correction for an array of spherical cavities in a soft medium.

Reference	Expression
Kobelev [38]	$I = 1 - 2(a/d_y)$
Leroy <i>et al.</i> [19]	$I = 1 - 2\sqrt{\pi}(a/d_y)$
Skvortsov <i>et al.</i> [20]	$I = (1 - \sigma^2)/(1 + 1.75\sqrt{\sigma} - 2.02\sigma^2)$, where $\sigma = \pi^3 a^2 / 4d_y^2$

cavity in an unbounded medium and cavities with lattice spacing equal to the diameter. In the limit $a/d_y = 0$, $I = 1$, which corresponds to monopole resonance of a single cavity. As a/d_y increases, i.e., cavities come closer to each other, I reduces and the resonance frequency increases as a consequence of resonance coupling [19]. The models for parameter I in the literature presented in Table I are valid for the filling fraction of cavities in a soft medium up to $a/d_y = 0.28$ [19] and $a/d_y = 0.36$ [20]. In contrast, the results for parameter I from Eq. (10) are valid for the entire range of a/d_y . Numerically, the resonance frequency of an array of inclusions corresponding

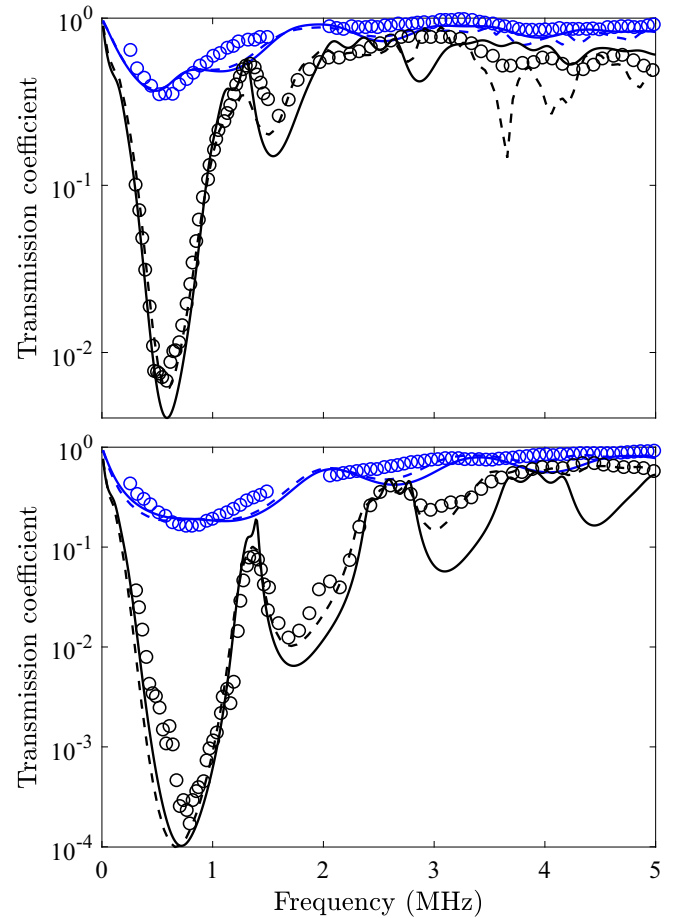


FIG. 3. Transmission coefficient of one layer (blue lines) and four layers (black lines) of spherical cavities embedded in a soft medium submerged in water, for low and moderate a/d_y values of 0.13 (top) and 0.19 (bottom) obtained using our analytical model (solid lines), numerical model (dashed lines), and experimental results from Leroy *et al.* [5] (circles).

to ω_0/\sqrt{I} was identified as the frequency of minimum sound transmission. Parameter I was obtained by repeating this procedure for a range of a/d_y values and using Eq. (1). Results obtained using Eq. (10) are in excellent agreement with numerical results for all a/d_y values.

We now present the transmission coefficient (ratio of the transmitted and incident pressures) of a soft medium embedded with one or four layers of evacuated spherical cavities of radius $38.5 \mu\text{m}$ and submerged in water. Within a layer, the cavities are arranged in a square lattice with a spacing of 300 or $200 \mu\text{m}$. These cases correspond to low and moderate a/d_y values of 0.13 and 0.19 , respectively. The spacing between the cavities in the direction of sound propagation is $360 \mu\text{m}$. The total thickness of the elastic medium in the direction of sound propagation for the models comprising one and four layers of cavities models is $720 \mu\text{m}$ and 1.8 mm , respectively. The centers of the cavities are $360 \mu\text{m}$ away from the interface between the host elastic medium and water on the incidence and transmission sides. The density and shear modulus of the host medium are 1000 kg/m^3 and $1.6(1+i) \text{ MPa}$. The sound speed and attenuation in the host medium are 1020 m/s and $4.6 \times 10^{-8} f^{1.45} \text{ m}^{-1}$, where f is the forcing frequency in Hz [5]. The first trough in the transmission coefficient for a single layer as well as four layers of cavities is due to monopole resonance of the cavities and its frequency can be predicted using ω_0/\sqrt{I} . The transmission coefficients for the $200 \mu\text{m}$ lattice spacing model are smaller compared to the $300 \mu\text{m}$ lattice spacing model, attributed to the stronger reflection of sound waves by a higher volume fraction of cavities in the elastic medium. Our analytical results are compared with numerical simulations as well as experimental results from Leroy *et al.* [5], showing excellent agreement in a broad frequency range that encompasses monopole resonance. Good agreement at higher frequencies is also achieved. To demonstrate the validity of our analytical model for a large a/d_y value, Fig. 4 presents the transmission coefficient of a

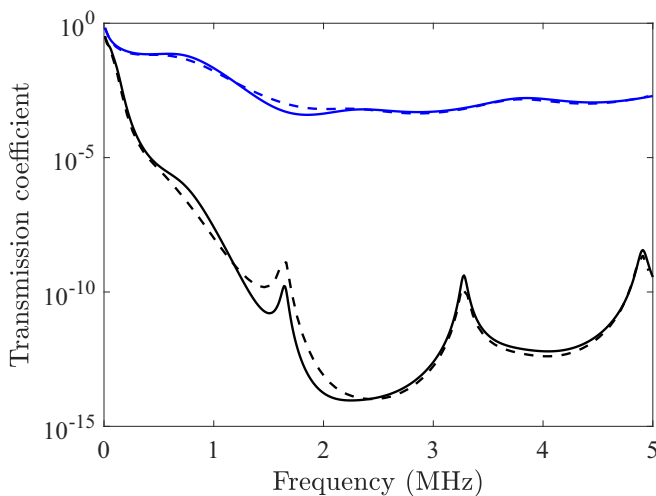


FIG. 4. Transmission coefficient of one layer (blue lines) and four layers (black lines) of spherical cavities embedded in a soft medium submerged in water, for a high a/d_y value of 0.45 obtained using our analytical model (solid lines) and numerical model (dashed lines).

soft medium embedded with one or four layers of cavities with a lattice spacing of $85.56 \mu\text{m}$. All other geometric and material parameters are the same as those used for Fig. 3. The a/d_y value for this case is 0.45 , which is very close to the full packing limit. Results obtained analytically and numerically are in excellent agreement, even at very low transmission

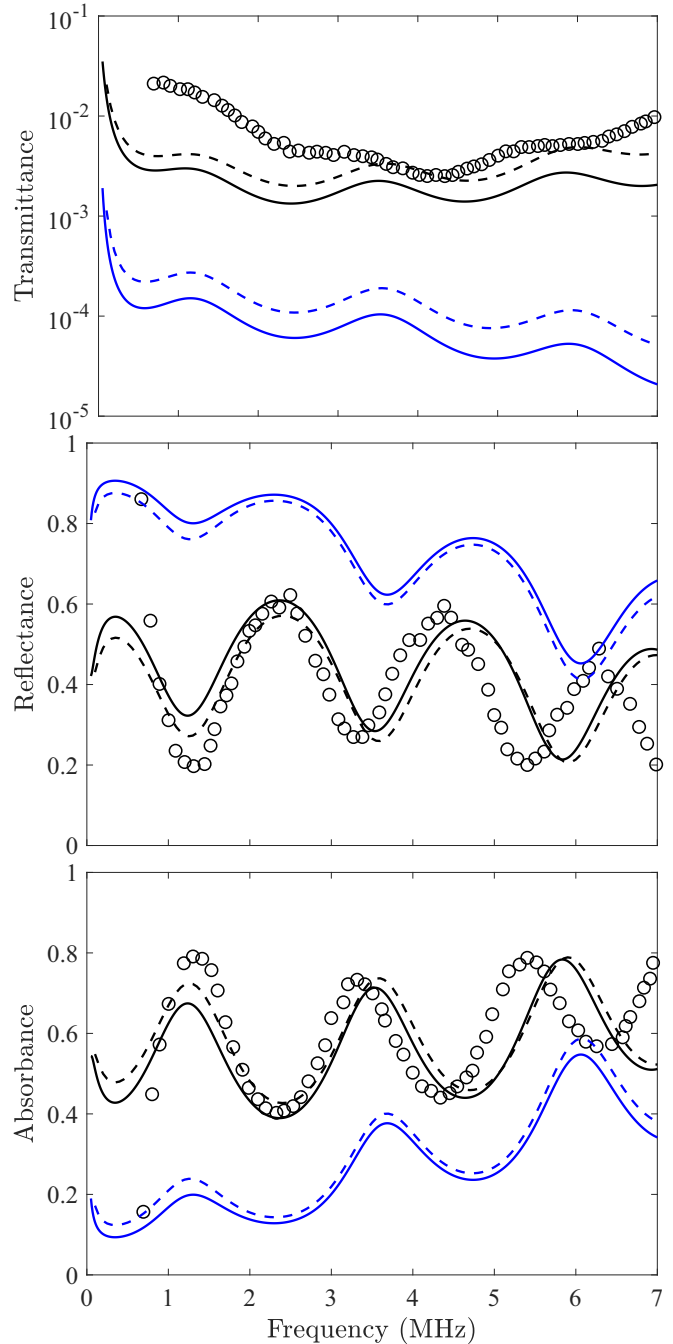


FIG. 5. Transmittance (top), reflectance (middle), and absorbance (bottom) of a layer of cavities embedded in a soft medium submerged in water and attached to a steel backing, for moderate and high a/d_y values of 0.22 (black lines) and 0.45 (blue lines) obtained using our analytical model (solid lines) and numerical model (dashed line). Experimental results from Leroy *et al.* [8] for $a/d_y = 0.22$ are also shown (black circles).

coefficient values. A comparison of Figs. 3 and 4 highlights that reducing cavity spacing significantly blocks the transmission of sound.

Next, we consider a metasurface submerged in water with a rigid backing on the transmission side. Figure 5 presents the transmittance (ratio of transmitted and incident acoustic energies), reflectance (ratio of reflected and incident acoustic energies), and absorbance of a single layer of cavities in a soft medium with water on the incidence side and steel on the transmission side. The cavities are of radius $11\ \mu\text{m}$ and arranged in a square lattice with a spacing of 50 or $24.44\ \mu\text{m}$. These cases correspond to moderate and high a/d_y values of 0.22 and 0.45 , respectively. The thickness of the elastic medium in the direction of sound propagation is $230\ \mu\text{m}$, with the cavities at a distance of $11\ \mu\text{m}$ from the steel backing. The density and shear modulus of the elastic medium are $970\ \text{kg/m}^3$ and $(0.6 + 7 \times 10^{-7}f) + i(0.2 + 1.8 \times 10^{-6}f)$ MPa. The sound speed and attenuation in the host medium are $1020\ \text{m/s}$ and $4.6 \times 10^{-8}f^{1.45}\ \text{m}^{-1}$. The layer of cavities generates reflected waves that have a phase difference of π compared to those reflected from the steel backing [8]. De-

structive interference of these two reflected waves leads to low sound reflection from steel covered with the metasurface. Further, high sound absorption by the metasurface is attributed to strong multiple scattering of waves between the cavities resulting in conversion of longitudinal waves into shear waves, which are subsequently dissipated in the elastic medium due to high shear damping. Our analytical and numerical results are in excellent agreement with the experimental results from Leroy *et al.* [8].

V. SUMMARY

We have presented an analytical framework based on an effective medium approximation to model sound scattering by a metasurface comprising a lattice of spherical inclusions in a soft medium. Our approach simplifies the analytical treatment of homogeneous media embedded with monopole scatterers while preserving the self-consistency of the original problem, and is valid for an extended range of the filling fraction of cavities including the closely spaced limit.

-
- [1] Y. Xie, W. Wang, H. Chen, A. Konneker, B.-I. Popa, and S. A. Cummer, *Nat. Commun.* **5**, 5553 (2014).
- [2] Y. Li, C. Shen, Y. Xie, J. Li, W. Wang, S. A. Cummer, and Y. Jing, *Phys. Rev. Lett.* **119**, 035501 (2017).
- [3] B. Assouar, B. Liang, Y. Wu, Y. Li, J.-C. Cheng, and Y. Jing, *Nat. Rev. Mater.* **3**, 460 (2018).
- [4] Y. Zhu and B. Assouar, *Phys. Rev. B* **99**, 174109 (2019).
- [5] V. Leroy, A. Bretagne, M. Fink, H. Willaime, P. Tabeling, and A. Tourin, *Appl. Phys. Lett.* **95**, 171904 (2009).
- [6] A. Bretagne, A. Tourin, and V. Leroy, *Appl. Phys. Lett.* **99**, 221906 (2011).
- [7] G. S. Sharma, A. Skvortsov, I. MacGillivray, and N. Kessissoglou, *Appl. Phys. Lett.* **116**, 041602 (2020).
- [8] V. Leroy, A. Strybulevych, M. Lanoy, F. Lemoult, A. Tourin, and J. H. Page, *Phys. Rev. B* **91**, 020301(R) (2015).
- [9] M. Lanoy, R.-M. Guillermic, A. Strybulevych, and J. H. Page, *Appl. Phys. Lett.* **113**, 171907 (2018).
- [10] M. Lanoy, R. Pierrat, F. Lemoult, M. Fink, V. Leroy, and A. Tourin, *Phys. Rev. B* **91**, 224202(R) (2015).
- [11] H. Ammari, B. Fitzpatrick, D. Gontier, H. Lee, and H. Zhang, *Proc. R. Soc. A: Math. Phys. Eng. Sci.* **473**, 20170469 (2017).
- [12] R. Sainidou, N. Stefanou, and A. Modinos, *Phys. Rev. B* **74**, 172302 (2006).
- [13] Z. Ye and A. Alvarez, *Phys. Rev. Lett.* **80**, 3503 (1998).
- [14] B. Liang and J.-C. Cheng, *Phys. Rev. E* **75**, 016605 (2007).
- [15] V. Leroy, A. Bretagne, M. Lanoy, and A. Tourin, *AIP Adv.* **6**, 121604 (2016).
- [16] H. Ammari, H. Lee, and H. Zhang, *SIAM J. Math. Anal.* **51**, 45 (2019).
- [17] J. Pierre, B. Dollet, and V. Leroy, *Phys. Rev. Lett.* **112**, 148307 (2014).
- [18] M. Lanoy, J. H. Page, G. Lerosey, F. Lemoult, A. Tourin, and V. Leroy, *Phys. Rev. B* **96**, 220201(R) (2017).
- [19] V. Leroy, A. Strybulevych, M. Scanlon, and J. Page, *Eur. Phys. J. E* **29**, 123 (2009).
- [20] A. Skvortsov, I. MacGillivray, G. S. Sharma, and N. Kessissoglou, *Phys. Rev. E* **99**, 063006 (2019).
- [21] P. Méresse, C. Audoly, C. Croënne, and A.-C. Hladky-Hennion, *Compt. R. Mecan.* **343**, 645 (2015).
- [22] M. Kafesaki, R. S. Penciu, and E. N. Economou, *Phys. Rev. Lett.* **84**, 6050 (2000).
- [23] O. Schnitzer, R. Brandão, and E. Yariv, *Phys. Rev. B* **99**, 195155 (2019).
- [24] H. Ammari and H. Zhang, *SIAM J. Math. Anal.* **49**, 3252 (2017).
- [25] A. N. Norris, *J. Acoust. Soc. Am.* **123**, 99 (2008).
- [26] P. A. Martin, *Multiple Scattering: Interaction of Time-harmonic Waves with N Obstacles* (Cambridge University Press, Cambridge, 2006), Vol. 107.
- [27] M. Yang, G. Ma, Y. Wu, Z. Yang, and P. Sheng, *Phys. Rev. B* **89**, 064309 (2014).
- [28] J.-J. Marigo and A. Maurel, *J. Acoust. Soc. Am.* **140**, 260 (2016).
- [29] V. Leroy, A. Strybulevych, J. H. Page, and M. G. Scanlon, *Phys. Rev. E* **83**, 046605 (2011).
- [30] D. V. Sivukhin, *Sov. Phys.-Acoust.* **1**, 82 (1955).
- [31] J. Sánchez-Dehesa and A. Krokhnin, in *Phononic Crystals* (Springer, New York, 2016), pp. 1–21.
- [32] P. A. Martin and R. A. Dalrymple, *J. Fluid Mech.* **188**, 465 (1988).
- [33] X. Cai and G. B. Wallis, *Phys. Fluids A: Fluid Dynam.* **4**, 904 (1992).
- [34] A. S. Sangani, D. Zhang, and A. Prosperetti, *Phys. Fluids A: Fluid Dynam.* **3**, 2955 (1991).
- [35] Y. Wu, Y. Lai, and Z.-Q. Zhang, *Phys. Rev. B* **76**, 205313 (2007).
- [36] L. L. Foldy, *Phys. Rev.* **67**, 107 (1945).

- [37] Z. Ye and L. Ding, *J. Acoust. Soc. Am.* **98**, 1629 (1995).
[38] Y. A. Kobelev, *Acoust. Phys.* **60**, 1 (2014).
[39] V. Fedotovskii and T. Vereschagina, *Acoust. Phys.* **56**, 506 (2010).
[40] N. Kanev, *Acoust. Phys.* **53**, 553 (2007).
[41] Z. Ye, *Acta Acust./Acust.* **89**, 435 (2003).
[42] G. S. Sharma, A. Skvortsov, I. MacGillivray, and N. Kessissoglou, *J. Acoust. Soc. Am.* **141**, 4694 (2017).